

ANALYSIS AND CALIBRATION OF QUINOA GRAIN PARAMETERS USED IN A DISCRETE ELEMENT METHOD BASED ON THE REPOSE ANGLE OF THE PARTICLE HEAP

/

基于堆积试验的藜麦离散元参数分析及标定

Fei Liu, Dapeng Li, Tao Zhang*, Zhen Lin¹

College of Mechanical and Electrical Engineering, Inner Mongolia Agricultural University, Hohhot / China

Tel: +86-471-5964308 E-mail: afei2208@imau.edu.cn

DOI: <https://doi.org/10.35633/inmateh-61-09>

Keywords: Quinoa, Discrete element method, Optimization, Parameter calibration, Repose angle

ABSTRACT

An optimization method based on a regression model was established by combining physical experiments, and an extended distinct element method (EDEM) simulation was proposed to address the difficult problem of obtaining the contact characteristic parameters used in the discrete element method (DEM) model of quinoa grains and for calibrating the parameters of the quinoa DEM model. The Plackett-Burman test was designed using Design-Expert software to screen the parameters of the quinoa DEM model, and the quinoa-quinoa static friction coefficient, quinoa-poly(lactic acid) (PLA) static friction coefficient and quinoa-quinoa rolling friction coefficient were found to have significant effects on the repose angle. The optimal value intervals of the parameters with a significant impact on the repose angle were determined using the steepest ascent test. A regression model of the repose angle and the parameters with a significant impact on the repose angle was then established with the Box-Behnken design and further optimized, and the combination of optimal parameters was as follows: 0.26 for the quinoa-quinoa static friction coefficient (E), 0.38 for the quinoa-PLA static friction coefficient (F), and 0.08 for the quinoa-quinoa rolling friction coefficient (G). Lastly, the optimal combination was used in the verification performed by the DEM simulation, and the error between the simulated repose angle and the target repose angle was 0.86%. These findings indicated that it was feasible to use the response surface optimization to calibrate the parameters required for quinoa DEM simulation and that the combination of optimal parameters can provide a reference for selecting the characteristic contact parameters used in quinoa DEM simulation.

摘要

针对藜麦离散元仿真模型接触参数难以直接获取的问题,提出一种结合物理试验和 EDEM 仿真试验建立回归模型进行寻优的方法,对藜麦离散元仿真模型参数进行标定。应用 Design Expert 软件设计 Plackett-Burman 试验对藜麦离散元模型参数进行筛选,得到藜麦-藜麦静摩擦系数、藜麦-PLA 静摩擦系数和藜麦-藜麦滚动摩擦系数对休止角影响显著;通过最陡爬坡试验确定显著性参数的最优值区间,然后根据 Box-Behnken 设计结果建立休止角与显著性参数的回归模型并对其进行优化,得到显著性参数的最佳组合为:藜麦-藜麦静摩擦系数为 0.26、藜麦-PLA 静摩擦系数为 0.38、藜麦-藜麦滚动摩擦系数为 0.08。最后将最佳参数组合进行离散元仿真验证,仿真休止角与目标休止角的相对误差为 0.86%,表明应用响应面优化标定藜麦离散元仿真中所需的参数是可行的;标定所得的最佳参数组合可为藜麦离散元仿直接触参数的选取提供参考。

INTRODUCTION

Quinoa is resistant to cold, drought, barren soil, and saline-alkaline soil and is thus highly suitable for cultivation in arid and semiarid plateau areas. Due to its complete and rich nutritional content, quinoa is regarded as one of most promising “superfoods” for ensuring global food security and human nutrition in the 21st century, according to the Food and Agriculture Organization of the United Nations (Chen *et al.*, 2018). However, quinoa is planted by the hole sowing method, at 5-8 grains per hole, leading to serious grain waste. Quinoa seedlings look very similar to those of *Chenopodium album*, a common field weed, and both plants belong to the *Chenopodiaceae* family, making it very difficult to control weeds and thus resulting in high labour costs.

¹ Fei Liu, A/Prof. Ph.D. Eng.; Dapeng Li, As Ph.D. Stud. Eng.; Tao Zhang, Lec. Ph.D. Eng.; Zhen Lin, As M.S. Stud. Eng.

The mechanization level involved in harvesting quinoa is low, and the use of traditional combines for grain crops leads to high grain loss and high levels of impurities, which are seriously hampering the healthy development of the quinoa industry. Therefore, it is of great practical significance to study key common issues in quinoa mechanization.

In recent years, the discrete element method (DEM) has been increasingly used in research and development (R&D) on agricultural equipment, and good results have been obtained. Investigating the parameters involved in the quinoa DEM simulation can help in the R&D of quinoa production equipment (Ucguł *et al.*, 2017; Ucguł and Saunders, 2020; Sun *et al.*, 2018; Zhao *et al.*, 2013). The characteristic physical parameters of quinoa grain include its intrinsic parameters and contact characteristic parameters, which can be obtained through direct measurement. In EDEM, the intrinsic parameters can directly adopt measured values, but the established model and the actual grains have specific differences with one another, causing a simulation distortion when using measured contact characteristic parameters directly. Therefore, it is necessary to calibrate the contact characteristic parameters of quinoa grains.

These characteristic parameters include the static friction coefficient, rolling friction coefficient, and collision restitution coefficient (Zeng *et al.*, 2017; Bart *et al.*, 2014; González *et al.*, 2012). Scholars in China and abroad have investigated the parameter measurements of DEM simulations extensively. Han *et al.* constructed a linear equation for the rolling friction coefficient and repose angle, and they simulated the heaping process for ellipsoidal particles using the DEM, performed virtual experimental calibration on the measured parameters of loose materials, and obtained the rolling friction coefficient of granular materials, thereby providing approximate numerical measurements (Han *et al.*, 2014). Using rice grains as an example, Jia *et al.* simulated rice grain heaping in a bottomless cylinder using DEM and MATLAB graphic image processing techniques, demonstrating that this method was suitable for measuring the repose angle of rice grains; they were able to predict the repose angle of ellipsoidal granular materials with known physical and mechanical parameters (Jia *et al.*, 2014).

In many cases, the response surface design is integrated into the calibration and optimization of particle parameters. Li *et al.* obtained the repose angle of wheat kernels using the cylindrical lifting method, established and optimized a second-order regression model of the repose angle based on the static friction coefficient and rolling friction coefficient by response surface design, and compared the measured values with the simulated ones for model verification, thus providing a reference for the parameter calibration of granular materials, such as wheat kernels, in DEM simulations (Li *et al.*, 2016). Based on the DEM, Santos *et al.* obtained the dynamic repose angle of dried cherry fruits using a central combination experimental design and a rotating drum test and calibrated the parameters needed in DEM simulations (Santos *et al.*, 2015).

In this study, by using the Plackett-Burman, steepest ascent, and Box-Behnken tests, we calibrated the contact characteristic parameters of quinoa grains and polylactic acid (PLA), a new biobased, biodegradable, renewable material used for 3D printing, in the DEM model. We obtained the combination of optimal parameters and verified this combination by comparing the simulated repose angle and the target repose angle to provide a reference for the parameter calibration of quinoa grains in the DEM simulation.

MATERIALS AND METHODS

Basic parameters of quinoa grains

The quinoa used in this study was “Mengli No. 1” that was harvested in Liangcheng County, Ulanqab City, Inner Mongolia, China, with a density of 870 kg/m³, a water content of 8%, and a thousand-kernel weight of 2.27-2.35 g. Using an outside micrometre with an accuracy of 0.01 mm, the average length, width, and thickness of the quinoa grains were determined to be 1.803, 1.711, and 1.150 mm, respectively, with a sphericity of 0.85.

Test method

We first measured the repose angle of the quinoa grain using the injection method during the physical test, in addition to the contact characteristic parameters (collision restitution coefficient, static friction coefficient and rolling friction coefficient) to determine the value ranges. We then constructed a simulation model using SolidWorks software, which was added to EDEM for simulation, and we screened the contact characteristic parameters of the quinoa grains used in the DEM simulation using the Plackett-Burman test to determine the parameters that significantly affected the repose angle. Using the steepest ascent test, we obtained the optimal value intervals of the parameters that were significantly affecting the repose angle. We further established a regression model of the repose angle for the quinoa grain heap and the parameters that

significantly affect the repose angle by performing an analysis of variance (ANOVA) as part of the Box-Behnken test, and the regression model was optimized to obtain the optimal value for each significant parameter. Lastly, we performed verification by simulation using the calibrated parameters and compared the deviation between the simulated repose angle and the actual repose angle to verify the accuracy of the calibrated parameters. The effects of the repose angles of different materials on the parameters of the DEM model vary; because the regression model that was established using the response surface analysis method is continuous, the optimum value obtained through the optimization is more accurate (Yuan *et al.*, 2018).

Parameter calibration process and analysis

Determination of the repose angle

During this study, we calibrated the contact characteristic parameters of the quinoa grain and PLA, a new biobased, biodegradable, and renewable 3D printing material. In reference to *Surface active agents – Powders and Granules – Measurement of angle of repose* (GB11986-89), the national standard (GB/T 16913.5-1997) and the existing literature (Peng *et al.*, 2018), the repose angle of the quinoa grains was measured by the injection method using FT-104B powder and a particle repose tester. The setup is shown in Fig. 1. To obtain accurate measurements and calibrated parameters, the funnel and the cylindrical chassis were manufactured with PLA by 3D printing. The inner diameter of the lower opening in the funnel was 10 mm; the diameter of the cylindrical chassis was 50 mm; and the distance between the lower opening of the funnel and the upper surface of the cylindrical chassis was 50 mm. During the measurement, the instrument was placed and levelled on the table and ensured the centre of the chassis and the centre of the funnel in the same axis through the alignment of the concentric circles on the chassis. Then, a specific amount of grain was weighed and poured into the funnel. The height of the heap was measured sometime after the grains stopped flowing. The repose angle of the quinoa grains was calculated using Eq. (1), and 10 measurements were averaged, for a repose angle of 28.14°.

$$\theta = \arctan \frac{2l}{R} \quad (1)$$

where: θ is the repose angle, [°];

R is the diameter of the cylindrical chassis, [mm];

l is the height of the heap, [mm].

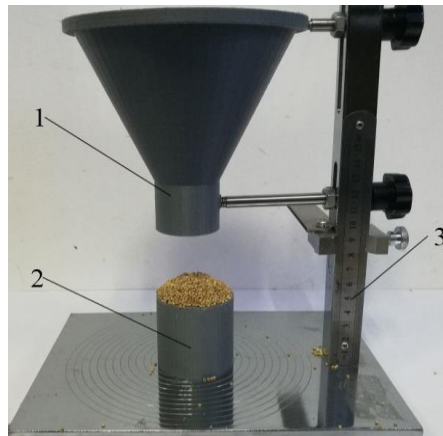


Fig. 1 - Angle of repose measuring instrument
1. PLA funnel; 2. PLA cylindrical chassis; 3. Iron stand

Determination of the friction coefficient

The friction coefficient was determined based on the inclined plane mechanics principle using the CNY-1 Inclined Plane Tester, as shown in Fig. 2. Because the grains roll on the plane, the quinoa grains were attached to the plane surface through adhesion, and the PLA plate and the adhesive plate for quinoa grains were used (Zhang *et al.*, 2017). The seeds are placed on the inclined surface, as the inclination angle of the inclined surface gradually increases, when the grain is just about to start sliding on the inclined surface, the inclination angle of the inclined surface at this moment is defined as static friction angle, and the corresponding static friction coefficient of the quinoa grain is calculated using Eq. (2), which is the friction

coefficient formula. The measurement was repeated 20 times, and the obtained average static friction coefficients were 0.468 between quinoa grains and 0.545 between quinoa grains and PLA.



Fig. 2 - Friction coefficient tester

$$\mu = \tan \beta \quad (2)$$

where: μ is the static friction coefficient, [-];
 β is the static friction angle, [°];

Similarly, to measure the rolling friction coefficient, a single quinoa grain was placed on the test material; when the grain was just about to roll, the inclination angle of the inclined surface was defined as the rolling friction angle of the grain, and the rolling friction coefficient of the grain was calculated using Eq. (2). The measurement was repeated 20 times, and the average rolling friction coefficients were 0.141 between quinoa grains and 0.124 between quinoa grains and PLA.

Determination of the restitution coefficient

The collision restitution coefficient reflects the ability of an object to retake its form following deformation during a collision, and it is only related to the materials in the collision. During testing, the grain was dropped and allowed to free-fall from fixed height H , and it collided with the test material to rebound. This process was videotaped with a camera using a test system, as shown in Fig. 3. After the test, the video was analysed and the grains that experienced a direct collision were analysed; rebounding height of the grain after its collision with the test material was determined. The restitution coefficient of quinoa grain was calculated using Eq. (3). The measurement was repeated 20 times, and the obtained average restitution coefficients were 0.347 between quinoa grains and 0.455 between quinoa grains and PLA.

$$e = \sqrt{\frac{h}{H}} \quad (3)$$

where: e is the restitution coefficient, [-];
 h is the seed bounce height, [mm];
 H is the seed falling distance, [mm].

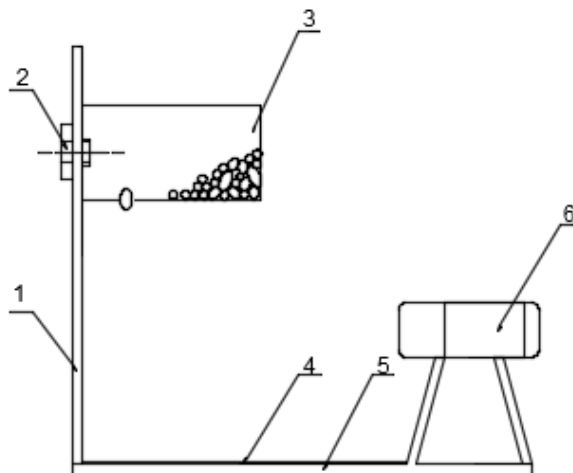


Fig. 3 - Collision recovery coefficient tester

1. Calibration plate 2. Fixed bolt 3. Blanking box 4. Test material plate 5. Base 6. Camera

DEM model of quinoa grains

Quinoa grains assume the form of a round tablet without an adhesive surface. For this study, we adopted the Hertz-Mindlin (no slip) contact model in the EDEM software and used the 6-ball combination method to construct a DEM model of the quinoa grains, as shown in Fig. 4. In the simulation model, the quinoa grain was 1.8 mm long, 1.7 mm wide, and 1.1 mm thick, with a relative size error of 1.57%.

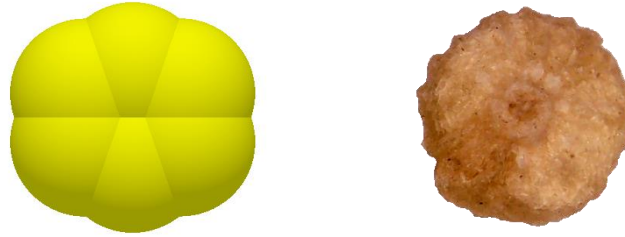


Fig. 4 - Quinoa seed particle model

Simulation parameters

By combining the existing physical characteristic parameters of the quinoa grain with the measured parameters, we determined the variation ranges of the simulation parameters, as shown in Table 1. During the simulation, we set the time step to 20% of the Rayleigh time step and the grid size to five times the minimum spherical element size.

Table 1

Parameters required in DEM simulation

Parameters	Value
Poisson's ratio of quinoa	0.2-0.3 ^a
Poisson's ratio of PLA	0.25-0.47 ^a
Young's modulus of quinoa [MPa]	390.00
Young's modulus of PLA [MPa]	2 350.00
Density of quinoa [kg·m ⁻³]	0.87
Density of PLA [kg·m ⁻³]	1.23
Quinoa-quinoa restitution coefficient	0.22-0.54 ^a
Quinoa-PLA restitution coefficient	0.32-0.68 ^a
Quinoa-quinoa static friction coefficient	0.24-0.70 ^a
Quinoa- PLA static friction coefficient	0.32-0.66 ^a
Quinoa-quinoa rolling friction coefficient	0.05-0.19 ^a
Quinoa- PLA rolling friction coefficient	0.03-0.19 ^a

Note: a shows the term is variable.

Simulation model of the repose angle

The Hertz-Mindlin (no slip) contact model in the EDEM software was adopted, and the inner diameters and heights of the funnel and the cylinder chassis were identical to those in the repose angle test, as shown in Fig. 5. The particles formed a particle plant at the top of the funnel. The Dynamic particle generation method was used, and 7,000 particles were generated. The fixed time step was 25% of the Rayleigh time step. After all the particles in the funnel fell into the chassis, they were left to rest for a period of time, a stable particle heap was formed on the chassis, and then the repose angle was measured.

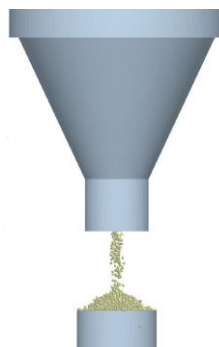


Fig. 5 - Simulation of quinoa seed particle accumulation

Response surface design for simulation parameters

To calibrate the repose angle parameters accurately, the grain contact characteristic parameters were screened based on their significance. In this study, the Plackett-Burman test was performed using Design-Expert 8.0.6 software, and eight true parameters and three virtual parameters, each having two levels (high and low), were chosen. The test parameters are shown in Table 2.

Table 2

Test parameters			
Symbol	Parameters	Low level	High level
A	Poisson's ratio of quinoa	0.2	0.3
B	Poisson's ratio of PLA	0.25	0.47
C	Quinoa-quinoa restitution coefficient	0.22	0.54
D	Quinoa-PLA restitution coefficient	0.32	0.68
E	Quinoa-quinoa static friction coefficient	0.24	0.70
F	Quinoa- PLA static friction coefficient	0.32	0.66
G	Quinoa-quinoa rolling friction coefficient	0.05	0.19
H	Quinoa- PLA rolling friction coefficient	0.03	0.19
J, K, L	Virtual parameters	-1	1

The Plackett-Burman test design designs were coded as -1 and +1, with one centre point, over a total of 13 tests. After the parameters with a significant impact on the repose angle were screened out using the Plackett-Burman test. The steepest ascent test was used to determine the optimal value interval for each parameter rapidly. Based on the steepest ascent test results and the response surface design principle, Box-Behnken test was performed and three levels, i.e., low (-1), medium (0) and high (1), were chosen for each parameter with a significant effect. The medium level was chosen for each parameter with a nonsignificant effect, and three centre points were designed to assess the error.

RESULTS AND DISCUSSION

Plackett-Burman test

The results are shown in Table 3. The ANOVA was performed on the test results using Design-Expert software, and the effect of each parameter is shown in Table 4, indicating that the quinoa-quinoa static friction coefficient (*E*), quinoa-PLA static friction coefficient (*F*) and quinoa-quinoa rolling friction coefficient (*G*) had a significant effect on the repose angle of the grains, while other parameters only had a nonsignificant effect. Thus, in the steepest ascent test and the Box-Behnken test, only the above three parameters with a significant impact were considered, and for the parameters with a nonsignificant effect, an intermediate value was chosen (i.e., the Poisson's ratio of quinoa: 0.25; the Poisson's ratio of PLA: 0.36; quinoa-quinoa restitution coefficient: 0.38; quinoa-PLA restitution coefficient: 0.50; and quinoa-PLA rolling friction coefficient: 0.11).

Table 3

Design and results of Plackett-Burman test												
No.	Test factors											Angle of repose [°]
	A	B	C	D	E	F	G	H	J	K	L	
1	1	-1	-1	-1	1	-1	1	1	-1	1	1	45.23
2	-1	1	1	-1	1	1	1	-1	-1	-1	1	36.34
3	1	1	-1	-1	-1	1	-1	1	1	-1	1	29.42
4	1	-1	1	1	1	-1	-1	-1	1	-1	1	30.46
5	0	0	0	0	0	0	0	0	0	0	0	38.38
6	1	1	1	-1	-1	-1	1	-1	1	1	-1	28.55
7	1	1	-1	1	1	1	-1	-1	-1	1	-1	34.22
8	-1	1	1	1	-1	-1	-1	1	-1	1	1	22.39
9	-1	-1	1	-1	1	1	-1	1	1	1	-1	35.60
10	-1	1	-1	1	1	-1	1	1	1	-1	-1	42.24
11	1	-1	1	1	-1	1	1	1	-1	-1	-1	33.42
12	-1	-1	-1	-1	-1	-1	-1	-1	-1	-1	-1	22.00
13	-1	-1	-1	1	-1	1	1	-1	1	1	1	33.58

Analysis of significance of parameters in Plackett-Burman test

Table 4

Parameters	Effect	Sum of squares	Contribution [%]	Significance
A	-0.14	0.06	0.01	8
B	0.48	0.69	0.10	7
C	-1.62	8.22	1.16	6
D	-1.80	9.77	1.38	5
E	10.79	349.16	49.14	1
F	3.62	39.28	5.53	3
G	9.21	254.56	35.82	2
H	2.19	14.41	2.03	4

Steepest ascent test

The results are shown in Table 5, and the results showed that as the *E*, *F*, and *G* increased, the repose angle gradually increased. The relative error was the lowest at Level 2, and it decreased first and then increased when changed from Level 1 to Level 3. This finding indicated that the optimal value interval was close to Level 2, which was then chosen as the centre point, and Levels 1 and 3 were designated as the low and high levels, respectively, to set up the subsequent response surface design.

Design and results of steepest ascent test

Table 5

No.	Test factors			Angle of repose [°]	Relative error [%]
	<i>E</i>	<i>F</i>	<i>G</i>		
1	0.2	0.31	0.04	21.41	23.93
2	0.3	0.38	0.07	28.72	2.07
3	0.4	0.45	0.10	37.23	32.32
4	0.5	0.52	0.13	41.35	46.94
5	0.6	0.59	0.16	44.07	56.60
6	0.7	0.66	0.19	45.57	61.93

Box-Behnken test

The Box-Behnken test results are shown in Table 6. A second-order regression model of the repose angle for parameters with a significant effect was established using Design-Expert software, and the quadratic polynomial equation is as follows:

$$\theta = -9.63 + 36.74E + 123.53 - 69.64G + 72.50 + 175.83EG + 101.19FG - 64.79E^2 - 169.98F^2 + 247.53G^2 \quad (4)$$

Design and results of Box-Behnken test

Table 6

No.	Test factors			Angle of repose [°]
	<i>E</i>	<i>F</i>	<i>G</i>	
1	-1 (0.20)	0(0.38)	-1(0.04)	23.56
2	1(0.40)	0	-1	30.46
3	0(0.30)	-1(0.31)	1(0.10)	28.72
4	-1	0	1	25.83
5	0	1(0.45)	1	32.13
6	-1	1	0(0.07)	25.27
7	1	1	0	33.42
8	0	0	0	29.07
9	0	0	0	28.90
10	0	1	-1	27.93
11	0	0	0	29.25
12	-1	-1	0	22.78
13	0	-1	-1	25.27
14	1	0	1	34.84
15	1	-1	0	28.90

The ANOVA results of the model are shown in Table 7. The *E*, *F*, *G*, and the quadratic term of *F* (F^2) showed a highly significant effect on the repose angle. The quadratic term of *E* (E^2) and the interaction terms of *E* and *F* (*EF*) and *E* and *G* (*EG*) showed a significant effect on the repose angle. The linear regression

model had a $P < 0.01$, indicating that the relationship of the repose angle with the obtained regression equation was statistically significant. The lack-of-fit item showed $P = 0.21 > 0.05$, indicating that the equation had a good fit. In the test, the coefficient of variation $CV = 1.30\%$, indicating that the test had high reliability. The determination coefficient $R^2 = 0.996$, the correction determination coefficient $R^2_{adj} = 0.989$, and the prediction determination coefficient $R^2_{pre} = 0.940$, all of which were close to 1, indicating that the model can truly reflect the actual situation. The test precision of Adep Precision = 39.962, indicating that the model had good accuracy.

ANOVA of quadratic polynomial model of Box-Behnken test

Table 7

Source of variation	Sum of squares	df	Mean square	P-value
Model	167.45	9	18.61	<0.0001
<i>E</i>	113.85	1	113.85	<0.0001
<i>F</i>	21.06	1	21.06	<0.0001
<i>G</i>	25.92	1	25.92	<0.0001
<i>EF</i>	1.03	1	1.03	0.0406
<i>EG</i>	1.11	1	1.11	0.0357
<i>FG</i>	0.18	1	0.18	0.3025
<i>E</i> ²	1.55	1	1.55	0.0200
<i>F</i> ²	2.56	1	2.56	0.0075
<i>G</i> ²	0.23	1	0.23	0.2555
Residual	0.68	5	0.14	
Lack of fit	0.62	3	0.21	0.1313
Pure error	0.06	2	0.03	
Total	168.13	14		

$R^2=0.996$; $R^2_{adj}=0.989$; $R^2_{pre}=0.940$; $CV=1.30\%$; Adep Precision=39.962

Based on the results in Table 7, under the objective of ensuring that the model was significant and the lack-of-fit term was not significant, the terms (*FG*, *G*²) without a significant effect on the repose angle were excluded and the ANOVA results of the optimized model are shown in Table 8. The lack-of-fit term showed $P = 0.135 > 0.05$, indicating that the equation fit well. In the test, $CV = 1.390\%$, indicating that the test had high reliability. The $R^2 = 0.994$, $R^2_{adj} = 0.987$, and $R^2_{pre} = 0.955$, indicating that the model can truly reflect the actual situation. The test precision of Adep Precision = 41.084, indicating that the model was improved after the optimization. The regression equation after optimization is as follows:

$$\theta = -14.25 + 37.88E + 133.56F + 7.25G + 72.50EF + 175.83EG - 66.69E^2 - 173.86F^2 \quad (5)$$

ANOVA of modified model of Box-Behnken test

Table 8

Source of variation	Sum of squares	Freedom	Mean square	P value
Model	167.04	7	23.86	<0.0001
<i>E</i>	113.85	1	113.85	<0.0001
<i>F</i>	21.06	1	21.06	<0.0001
<i>G</i>	25.92	1	25.92	<0.0001
<i>EF</i>	1.03	1	1.03	0.0396
<i>EG</i>	1.11	1	1.11	0.0318
<i>E</i> ²	1.65	1	1.65	0.0139
<i>F</i> ²	2.70	1	2.70	0.0042
Residual	1.09	7	0.16	
Lack of fit	1.03	5	0.21	0.1347
Pure error	0.06	2	0.03	
Total	168.13	14		

$R^2=0.994$; $R^2_{adj}=0.987$; $R^2_{pre}=0.955$; $CV=1.39\%$; Adep Precision=41.084

Analysis of the interaction terms in the regression model

The ANOVA results of the optimized regression model indicated that two interaction terms, i.e., *EF* and *EG*, had a significant effect on the repose angle of the quinoa grains ($P < 0.05$). When *G* was 0.07 and *F* was 0.38, the response surfaces of three parameters (*E*, *F*, and *G*) under the interactions of *EF* and *EG* were plotted using Design-Expert software, as shown in Fig. 6, to describe the effect of the interaction term on the

repose angle in a visual manner. Fig. 6A and Fig. 6B show that compared to those of F and G , the response surface of E was steeper, indicating that it had a more profound effect on the repose angle.

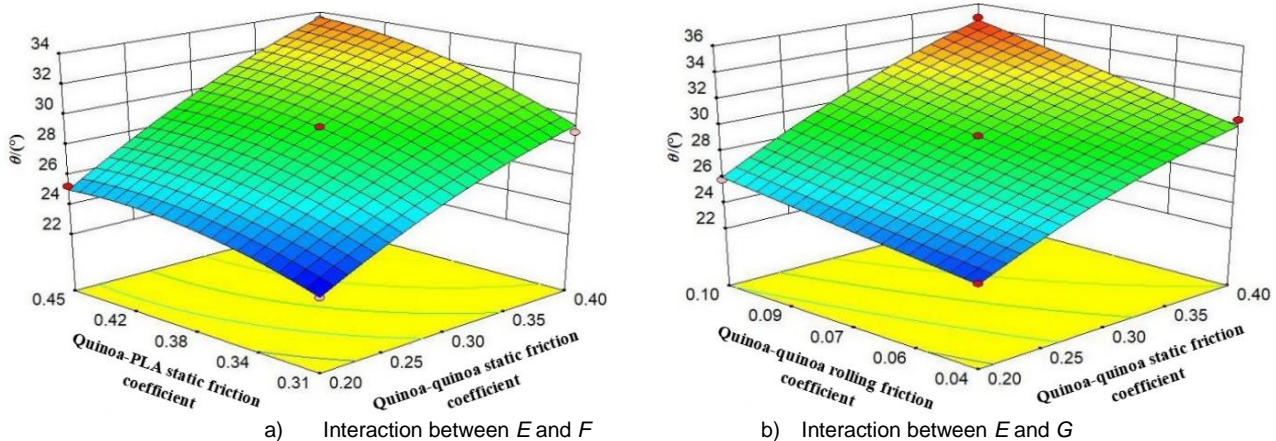


Fig. 6 - Interaction effect diagram of EF and EG

Determination of the optimal parameter combination and its simulation verification

With Design-Expert software, the optimized regression equation was solved with the actual repose angle of quinoa grains as the target, and the results showed that when E , F , and G were 0.26, 0.38, and 0.08, respectively, and the parameters with a nonsignificant effect were set to the medium level, the minimal deviation between the simulated repose angle and the experimental repose angle was obtained. The simulation on the repose angle was then performed with the combination of the above optimal parameters, and the comparison of the simulation and physical test is shown in Fig. 7. The repose angle values obtained through three repeated simulations were 28.55° , 28.05° , and 28.37° , with an average error of 0.86%, indicating the feasibility of the optimization of physical characteristic parameters for the quinoa grains used in the simulation by combining the significance analysis and the response surface method.



Fig. 7 - Comparison of simulation and physical tests

CONCLUSIONS

In this study, based on the reported experiments, we calibrated and optimized the simulation parameters of quinoa grains and the 3D printing material PLA using the DEM. Using Design-Expert software with the significance analysis and the response surface methods, we optimized and solved the simulation parameters with the repose angle as the response value, screened those with a significant impact on the repose angle, determined the optimum value range for each parameter, established a regression model, and analysed the interactions between the parameters to determine the optimal parameters. We then verified the accuracy of the quinoa grain simulation model through the simulation and drew the following conclusions:

1) The Plackett-Burman test results showed that E , F , and G had a significant effect on the repose angle, while the other parameters showed no significant impact on the repose angle of the quinoa grains.

2) The optimal value interval of the parameters with a significant effect on the repose angle was determined through the steepest ascent test. Based on the Box-Behnken test results, a second-order regression model of the repose angle on the parameters with a significant impact was established and optimized. The ANOVA results for the optimized model showed that in addition to the linear terms of the three parameters with a significant impact on the repose angle (E , F , and G), the interaction terms EF and EG and the quadratic terms F^2 and E^2 showed a significant effect on the repose angle.

3) The above regression equation was optimized and solved using the actual repose angle of quinoa grains as the target value, and the combination of the optimal parameters with a significant effect was obtained, i.e., E was 0.26, F was 0.38, and G was 0.08. The experimental comparison showed that the repose

angle obtained from the simulation was not significantly different from the actual repose angle ($P > 0.05$), indicating that the response surface analysis was feasible for calibrating the parameters used in the DEM simulation.

4) A simulation on the repose angle was performed using the obtained combination of optimal parameters, and the repose angle of the quinoa grains obtained through the simulation was 28.32° , which had an error of 0.86% under the experimentally measured repose angle (28.14°) and was not significantly different, indicating that the contact characteristic parameters obtained during the calibration can be used in the DEM simulation.

ACKNOWLEDGEMENT

The authors were funded for this project by Supported by Programme for Young Talents of Science and Technology in Universities of Inner Mongolia Autonomous Region (No. NJYT-20-B03).

REFERENCES

- [1] Guang Chen, Yang Sun, Gang Wang, Huan Chen, Shanshan Tang, Xiaoxiao Yu. (2018). Comprehensive utilization and development prospect of whole-plant chenopodium quinoa. *Journal of Jilin Agricultural University*, Vol. 40, issue 1, pp. 1-6;
- [2] Ucgul, M., Saunders C., Fielke, J. M. (2017). Discrete element modelling of tillage forces and soil movement of a one-third scale mouldboard plough. *Biosystems Engineering*, Vol 155, issue 3, pp. 44-54;
- [3] Ucgul, M., Saunders, C. (2020). Simulation of tillage forces and furrow profile during soil-mouldboard plough interaction using discrete element modelling. *Biosystems Engineering*, Vol190, issue 2, pp.58-70;
- [4] Zhao Z., Li Y., Liang Z., Gong Z. (2013). DEM simulation and physical testing of rice seed impact against a grain loss sensor. *Biosystems Engineering*, Vol 116, issue 4, pp. 410-419;
- [5] Sun J., Wang Y., Ma Y., Tong J., Zhang Z. (2018). DEM simulation of bionic subsoilers (tillage depth > 40 cm) with drag reduction and lower soil disturbance characteristics. *Advances in Engineering Software*, Vol 119, issue 5, pp. 30-37;
- [6] González-Montellano, C., Fuentes, J. M., Ayuga-Téllez, E., Ayuga, F. (2012). Determination of the mechanical properties of maize grains and olives required for use in DEM simulations. *Journal of food engineering*, Vol 111, issue 4, pp. 553-562;
- [7] Zeng Z., Chen Y., Zhang X. (2017). Modelling the interaction of a deep tillage tool with heterogeneous soil. *Computers & Electronics in Agriculture*, Vol 143, issue 12, pp. 130-138;
- [8] Lenaerts, B., Aertsen, T., TijskensE, Ketelaere B. D., Ramon, H., Baerdemaeker, J. D., Saeys, W. (2014). Simulation of grain–straw separation by Discrete Element Modeling with bendable straw particles. *Computers & Electronics in Agriculture*, Vol 101, issue 2, pp. 24-33;
- [9] Yanlong Han, Fuguo Jia, Yurong Tang, Yang Liu, Qiang Zhang. (2014). Influence of granular coefficient of rolling friction on accumulation characteristics. *Acta Physica Sinica*, Vol 63 , issue 17, pp. 173-179;
- [10] Fuguo Jia, Yanlong Han, Yang Liu, Yiping Cao, YuFei Shi, Lina Yao, Hui Wang. (2014). Simulation prediction method of repose angle for rice particle materials. *Transactions of the Chinese Society of Agricultural Engineering*, Vol 30, issue 11, pp. 254-260;
- [11] Fanyi Li, Jian Zhang, Bo Li, Jun Chen. (2016). Calibration of parameters of wheat required in discrete element method simulation based on repose angle of particle heap. *Transactions of the Chinese Society of Agricultural Engineering*, Vol 32, issue 12, pp. 247-253;
- [12] Santos, K.G., Campos, A.V.P., Oliveira, O.S, Ferreira L.V. (2015). Dem simulations of dynamic angle of repose of acerola residue: a parametric study using a response surface technique. *Blucher Chemical Engineering Proceedings*, Vol 1, issue 2, pp. 11326–11333;
- [13] Quanchun Yuan, Liming Xu, Jiejie Xing, Zhuangzhuang Duan, Shuai Ma, Changchang Yu, Chen. (2018). Parameter calibration of discrete element model of organic fertilizer particles for mechanical fertilization. *Transactions of the Chinese Society of Agricultural Engineering*, Vol 34 , issue 18, pp. 21-27;
- [14] Fei Peng, Hongying Wang, Fang, Yude Liu. (2018). Calibration of Discrete Element Model Parameters for Pellet Feed Based on Injected Section Method. *Transactions of the Chinese Society for Agricultural Machinery*, Vol 49, issue 4, pp. 140-147;
- [15] Tao Zhang, Fei Liu, Manquan Zhao, Yueqin Liu, Fengli Li, Qian Ma, Yong Zhang, Peng Zhou. (2017). Measurement of physical parameters of contact between soybean seed and seed metering device and discrete element simulation calibration. *Journal of China Agricultural University*, Vol 22 (9), pp. 86-92.